

Theme 02-1-1086-2009/2024

Strangeness in nucleon and nuclei

The HyperNIS project

Report on 2019-2021 upgrade of the spectrometer,
proposal for experiments in 2022-2024

*V.D.Aksinenko, A.V.Averyanov, A.E.Baskakov, S.N.Bazylev, V.F.Chumakov,
D.V.Dementiyev, A.A.Fechtchenko, A.A.Fedyunin, I.A.Filippov, S.V.Gertsenberger,
A.M.Korotkova, D.O.Krivenkov, R.I.Kukushkina, J.Lukstins, A.I.Maksimchuk,
O.V.Okhrimenko, A.N.Parfenov, N.G. Parfenova, S.N.Plyashkevich, P.A.Rukoyatkin,
R.A.Salmin, A.Sheremetiev, A.V.Shipunov, M.Shitenkov, A.V.Shutov, I.V.Slepnev,
V.M.Slepnev, E.A.Strokovsky, A.L.Voronin*

(VBLHEP JINR)

S.V.Tereschenko, V.V.Tereschenko

(DLNP JINR)

Czech Technical University, Prague, Czech Republic

S. Pospisil, J.Smejkal, V. Sopko, P. Manek

Institute of Experimental and Applied Physics (IEAP), Czech Technical University
Prague, Czech Republic

P.I.Kharlamov, M.G.Korolev, M.M.Merkin

SINP Lomonosov Moscow State University,

T.Nakano, M.Yosoi

RCNP, Osaka University Japan

Project leaders E.A.Strokovsky, J.Lukstins

Abstract

The experimental program of the HyperNIS project is aimed at investigation of the role which strangeness plays in nuclei (open strangeness in hypernuclei) and in nucleon (correlated $\bar{s}s$ pair, i.e. hidden intrinsic strangeness). Initially the program consisted, respectively, of two parts to be realized with the HyperNIS spectrometer. Taking into account spectrometer capacity our efforts are concentrated on hypernuclear research.

The first part of the program is aimed at study of the lightest neutron-rich hypernuclei; in particular, it is necessary to establish firmly if the hypernucleus ${}^6_{\Lambda}\text{H}$ really exists. It should be noted that in the same experiment the lifetimes and production cross sections of ${}^4_{\Lambda}\text{H}$ and ${}^3_{\Lambda}\text{H}$ will be investigated. If the existence of ${}^6_{\Lambda}\text{H}$ confirmed it will be naturally to push forward investigation of ${}^6_{\Lambda}\text{H}$ properties and the search for ${}^8_{\Lambda}\text{H}$, the most neutral nucleus among relatively heavy and complicated nuclei. The further experiment will be the study of ${}^6_{\Lambda}\text{He}$, previously observed only in emulsion experiments. The next step of this program is aimed to determine the binding energy of the loosely bound ${}^3_{\Lambda}\text{H}$ hypernucleus.

Upgrade of the spectrometer is done: new readout electronics is elaborated and installed, as well as new power supply modules for proportional chambers. RPC wall installed for TOF measurements (slow pions), all modules of VME crate (TQDC, synchronization) are new as well as server, trigger modules, high voltage and gas supply systems. The spectrometer is ready for experiments.

1 Introduction

The project is aimed to study the lightest neutron-rich hypernuclei; in particular, to search for (study of) ${}^6_{\Lambda}\text{H}$. Simultaneously, the lifetimes and production cross sections of ${}^4_{\Lambda}\text{H}$ and ${}^3_{\Lambda}\text{H}$ will be studied in the same experiment because we will use reaction ${}^7\text{Li} + \text{C} \rightarrow {}^A_{\Lambda}\text{H} + \text{K} + \text{p(d,t,n)} + \dots \rightarrow {}^A\text{He} + \pi^- + \dots$ (where $A=3,4,6$). Moreover, production of ${}^4_{\Lambda}\text{H}$ and ${}^3_{\Lambda}\text{H}$ hypernuclei is the precise reference signal to make sure that ${}^6_{\Lambda}\text{H}$ should be seen or that there are no stable forms of ${}^6_{\Lambda}\text{H}$ if it is not observed in the same run. This task is regarded as the very first experiment because at Frascati experiment [1, 2, 3] evidence of only three events was reported and controversial data obtained at J-PARC [4], where no signal was detected (instead of expected 50 events). On the other hand, before the J-PARC experiment A.Gal predicted that the possibility to see ${}^6_{\Lambda}\text{H}$ signal was low in the case because the spectrometer at J-PARC is not suited well for the task – the energy of recoil nuclei is too high while pion beam produces hypernuclei of high excitation levels maybe impossible in case of low hypernucleus binding energy. Moreover, to produce ${}^6_{\Lambda}\text{H}$ using ${}^6\text{Li}$ target double charge exchange reaction is necessary. The process is suppressed and a lot of uncertainties should be solved to predict production rate.

The result of ${}^6_{\Lambda}\text{H}$ hypernucleus search should be a turning point of our program. If ${}^6_{\Lambda}\text{H}$ production cross section is high enough and event yield is large one should choose between two ways – either to continue the study of ${}^6_{\Lambda}\text{H}$ properties or to search for ${}^8_{\Lambda}\text{H}$ hypernucleus. It seems the search for and possible discovery of ${}^8_{\Lambda}\text{H}$ hypernucleus will be the best decision. Particularly since it is very difficult task to investigate ${}^8_{\Lambda}\text{H}$ using pion or kaon beams. The results of these two experiments will determine if it is useful to study properties of the new hypernuclei or to turn to ${}^6_{\Lambda}\text{He}$ and ${}^3_{\Lambda}\text{H}$ hypernucleus program.

The study of poorly investigated hypernucleus ${}^6_{\Lambda}\text{He}$ will be a natural continuation of Li beam experiments. With carbon beams the program can be extended by determination of the $\Lambda\text{N} \rightarrow \text{NN}$ weak interaction effective Hamiltonian.

Original and attractive idea is the experimental estimation of the binding energy of the loosely bound ${}^3_{\Lambda}\text{H}$ hypernucleus. Here the approach suggested in the Laboratory of High Energies (JINR, Dubna) will be used. In this approach the hypernuclei under study are being produced by the excitation of the beam nuclei and the hypernuclei decay is being observed at a distance of tens of centimeters behind the production target. Thus, passage of the hypernuclei “beam” through materials with different Z can be investigated in order to obtain experimental estimation of the ${}^3_{\Lambda}\text{H}$ binding energy. However, the best source of ${}^3_{\Lambda}\text{H}$ beam is primary ${}^4\text{He}$ beam. This experiment will be

done in perspective but beyond the 2022-2024 time schedule.

2 Physics motivation

The Hypernuclear program at Dubna [5, 6] was started in 1988 with the setup based on 2-m streamer chamber. The investigation of the light hypernuclei production and decay [7] was done, namely, the lifetime of ${}^4_{\Lambda}\text{H}$ and ${}^3_{\Lambda}\text{H}$ as well as their production cross sections were measured. It was shown that the approach, in which the momentum of hypernuclei produced in the beams of relativistic ions is close to the momentum of the projectiles, was quite effective for measurements of hypernuclei lifetimes and production cross sections. The dedicated and very selective trigger on two body hypernuclei decays with negative pion was the key point of this approach. The accuracy of lifetime measurements was, therefore, restricted only by statistical errors. The values of the experimental cross section were in good agreement with the results of the calculations (refs. [8] of H.Bandō, M.Sano, J.Žofka and M.Wakai, see also review [9]) performed using the coalescence model. It should be noted that hypernucleus lifetime up to now remains an actual problem. At the Conference HYP2015 on hypernuclear physics (Sendai, Japan, 2015) there was a special section organized to discuss light hypernuclei low lifetime puzzle. Most of the measurements [10, 11, 12] have shown ${}^3_{\Lambda}\text{H}$ lifetime values of 140-200 ps (155ps at STAR, 181ps at ALICE) while theory predicts 240-260 ps (256 ps, H.Kamada [13], 233-244 ps, T.Motoba [14]). For example, see Fig. 1. At the next Conference controversial ${}^3_{\Lambda}\text{H}$ lifetime results were reported by ALICE $\tau = 223^{+41}_{-33}(\text{stat.}) \pm 20(\text{syst.})\text{ps}$ [15] and STAR $\tau = 142^{+24}_{-21}(\text{stat.}) \pm 29(\text{syst.})\text{ps}$ [16]. See Fig. 2.

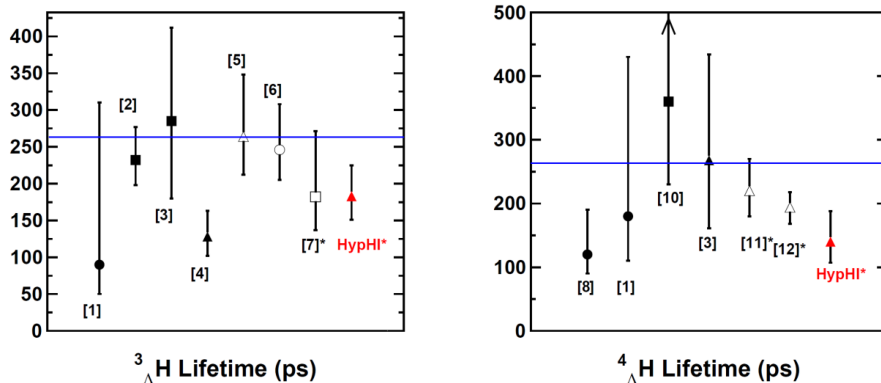


Figure 1: World data comparison of ${}^3_{\Lambda}\text{H}$ and ${}^4_{\Lambda}\text{H}$ lifetimes presented by Rappold in Proceedings [12] where references are listed. It should be said that ${}^4_{\Lambda}\text{H}$ lifetime value noted as [11] is result of our previous experiment [17]. Values deduced in the HypHI experiment are indicated by "HypHI". The horizontal line at 263.2 ps shows the known lifetime of the Λ hyperon. References to counter experiments are marked by an asterisk.

In all the previous hypernuclei experiments (except the above mentioned Dubna experiments and the Heavy Ion Beam experiment at GSI, Darmstadt [18, 19]) the hypernuclei are produced in various processes of target excitation. Common feature

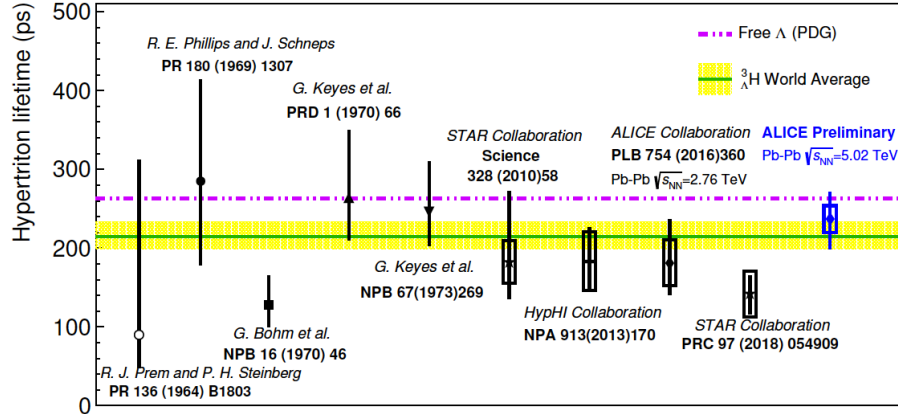


Figure 2: One can see that 3 years later STAR result is low while ALICE measurement gives much higher value. Presented by ALICE team at HYP2018 Conference [15].

of all such experiments is that momenta of the produced hypernuclei are low and they decay practically at the production point inside the target. On the contrary, in Dubna experiments [20] the energy of hypernuclei is only slightly lower than that of the beam nuclei (see Fig. 3). Therefore the hypernuclei lifetime in the laboratory reference frame is increased by the Lorentz factor 3-7, and significant part of hypernuclei decays far behind the production target. Thus, the location of the decay vertices can be used for identification of the hypernuclei decay and for determination of the lifetime of the observed hypernuclei by measurements of their flight path distribution.

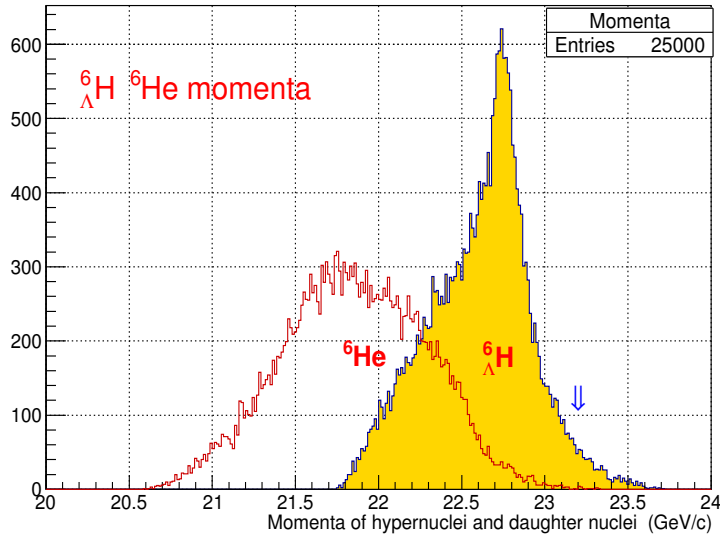


Figure 3: Expected distribution of ${}^6_{\Lambda}\text{H}$ hypernuclei and daughter He momenta. Arrow shows beam momentum (23.2 GeV/c). Due to Fermi motion and beam fragmentation momenta of few hypernuclei is higher than mean momentum value for 6 nucleons (${}^7\text{Li}$ beam).

The HyperNIS program is focused on **properties of the neutron rich halo**

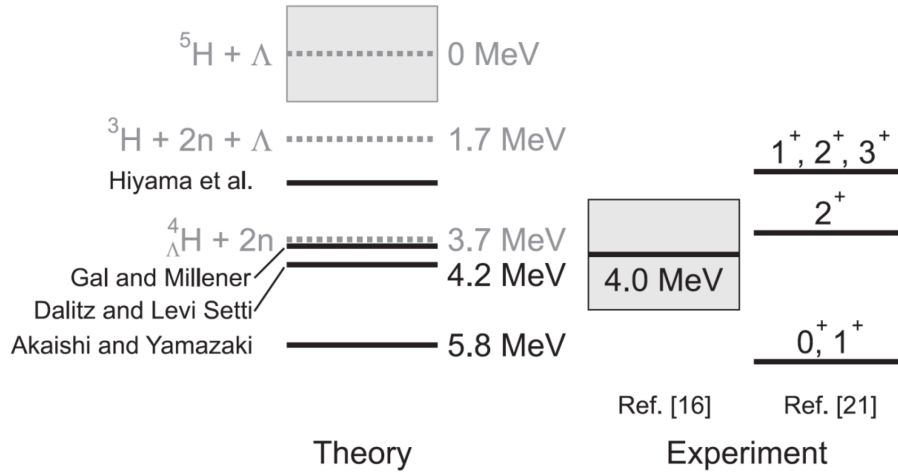


Figure 4: A summary of energy levels of ${}^6_{\Lambda}\text{H}$. Right side shows energy levels and binding energies reported by the FINUDA collaboration in Refs. [1, 2], and left side shows theoretically calculated binding energies from Refs. [25, 26, 27, 28]. All the binding energies are measured from the ${}^5\text{H} + \Lambda$ threshold.

hypernuclei. In the last time, properties of neutron rich hypernuclei and double hypernuclei are highly anticipated to revise theory (EOS) of neutron stars to solve hyperon puzzle in the case. Barion energy distribution in neutron stars predicts that a part of barions should be Lambda particles but Lambdas can change most of temporary suggestions for EOS so that 1.4–1.5 of Solar masses should be limit of a neutron star while mass of two of them is equal 2 Solar masses [21]. Recently, theory suggest how to solve problem [22] but new hypernuclear experimental data will help to choose the proper way.

First of all, study of the ${}^6_{\Lambda}\text{H}$ hypernucleus will be carried out with the ${}^7\text{Li}$ beam:

$${}^7\text{Li} + C \rightarrow {}^A_{\Lambda}\text{H} + p(d, t, n) + \dots \rightarrow {}^A\text{He} + \pi^- + \dots \quad \text{where } A=3,4,6. \quad (1)$$

We have chosen the ${}^7\text{Li}$ beam because an extra proton from the ${}^7\text{Li}$ can be stripped by fragmentation while additional charge exchange reaction is necessary if a ${}^6\text{Li}$ beam is used to produce the ${}^6_{\Lambda}\text{H}$ hypernucleus. Probability of fragmentation is much higher than that of charge exchange reaction. Some discussion of double charge exchange problem considering ${}^6_{\Lambda}\text{H}$ hypernucleus production is presented, for example, by A.Sakaguchi [23].

An evidence from Frascati for three ${}^6_{\Lambda}\text{H}$ hypernuclei was reported [1, 2]. In the concluding remarks at the closing of the 11th International Conference on Hypernuclei and Strange Particle Physics (held in 2012 in Barcelona) the first observation of ${}^6_{\Lambda}\text{H}$ was mentioned by T.Nagae [24] as one of the four main achievements in hypernuclear physics reached during the last years. On the other hand, the E10 collaboration at J-PARC experiment did not observe missing mass peak corresponding to ${}^6_{\Lambda}\text{H}$ production [4, 23]. However, A.Gal at the Barcelona Conference discussion noted, that there will be low probability to see signal from ${}^6_{\Lambda}\text{H}$ at J-PARC experiment due to high transferred momentum and, consequently, high momentum and excitation of produced

hypernuclei. Theoretical predictions are strongly model dependent and are controversial as well. For example, E.Hiyama and others have calculated [28] that ${}^6_{\Lambda}\text{H}$ is not stable nucleus and should decay into ${}^4_{\Lambda}\text{H}+n+n$ if one takes into account the parameters of ${}^5\text{H}$ resonance measured up to now. At the same time there are estimates [29, 30] showing that the binding energy for ${}^6_{\Lambda}\text{H}$ should be about a few MeV. So, it is necessary to carry out an experiment what can test ${}^6_{\Lambda}\text{H}$ hypernucleus without doubt. At J-PARC the search for ${}^6_{\Lambda}\text{H}$ was continued as the phase-1 of the J-PARC E10 experiment what was performed at the J-PARC 50 GeV proton-synchrotron facility. However, the search for ${}^6_{\Lambda}\text{H}$ by the ${}^6\text{Li}(\pi^-, \text{K}^+)$ reaction at the pion beam momentum of 1.2 GeV/c gave no events again [23]. Considering theory it should be cited A.Sakaguchi [23] at Sendai Conference:

“The results of the theoretical calculations indicate that the binding energy of ${}^6_{\Lambda}\text{H}$ is sensitive to the interactions and the models employed in the calculations and also the structure of the ${}^5\text{H}$ nucleus. The FINUDA collaboration also made another assignment of the 3 candidate events in which the 3 events of ${}^6_{\Lambda}\text{H}$ corresponded to different states as shown in the most right part in Fig. 3 (we present this Figure from Sakaguchi paper as Fig. 4). The level structure of ${}^6_{\Lambda}\text{H}$ still has ambiguities only with the FINUDA result, and complementary measurements are necessary (we emphasize this statement). The production mechanism by the DCX (double charge exchange) reaction and the structure of the neutron-rich ${}^6_{\Lambda}\text{H}$ hypernuclei are not well understood, yet. More detailed analysis of the already obtained experimental data and further experimental studies of other neutron-rich ${}^6_{\Lambda}\text{H}$ hypernuclei are necessary.”

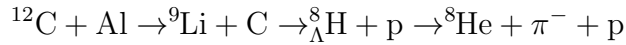
Anyway, it seems that if pion beams are used, ${}^6_{\Lambda}\text{H}$ production cross section is tiny and more precise experiments with pion beams will be difficult. On the contrary, we suggest to use ${}^7\text{Li}$ fragmentation due to much higher reaction probability instead of DCX of ${}^6\text{Li}$.

At this point one should note that in Frascati and J-PARC experiments no hypernuclei were directly observed, only secondary effects like negative pions assumed as products of ${}^6_{\Lambda}\text{H}$ decay or missing mass of possible production reaction were determined. Because statistics at Frascati was very low (3 candidates), while no signal at J-PARC was observed, the situation is controversial. Therefore a crucial experiment can be carried out at the VBLHEP of JINR. Search for ${}^6_{\Lambda}\text{H}$ with HyperNIS spectrometer to obtain high enough statistics (few hundreds of detected events) should be done in order to measure lifetime and production cross sections. That will provide a basis to solve the problem: whether hyperons indeed are acting as a “glue” in the vicinity of the neutron rich drip line. Also, the mass of isotope ${}^6_{\Lambda}\text{H}$ can be measured with use of our magnetic spectrometer.

Actually, in the Dubna experiment three isotopes of hydrogen hypernuclei (${}^3_{\Lambda}\text{H}$, ${}^4_{\Lambda}\text{H}$, ${}^6_{\Lambda}\text{H}$) should be produced simultaneously. It must be stressed that ${}^3_{\Lambda}\text{H}$ and ${}^4_{\Lambda}\text{H}$ can be used as a “reference points” to confirm the production and decay of ${}^6_{\Lambda}\text{H}$. Of course, lifetimes of all these hypernuclear isotopes can be measured as well.

Production of hypernuclei with a large neutron excess and a neutron halo was discussed by L.Majling since 1994 [31, 32]. Possibility to study baryon-baryon interaction

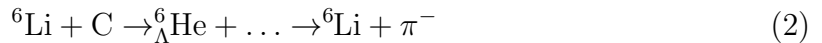
in system with extremely large value of $N/Z=6$ was pointed out. It was also emphasized that measurement of ${}^6_{\Lambda}\text{H}$ mass allows verification of the assumption that binding energy in neutron rich hypernuclei should be increased due to a specific “coherent $\Lambda - \Sigma$ mixing mechanism” [33, 34]. It should be noted that there is a chain of four nuclei with two neutron halo and different composition of the S -shell core: with and without Λ hyperon, namely the nuclei ${}^5\text{H}$, ${}^6_{\Lambda}\text{H}$, ${}^6\text{He}$, ${}^7_{\Lambda}\text{He}$. Thus, study of the ${}^6_{\Lambda}\text{H}$ properties (as well as of ${}^6_{\Lambda}\text{He}$) will be significant for the theory. Also it was noted that a ${}^8_{\Lambda}\text{H}$ hypernucleus can be possible. If the first experiment with ${}^6_{\Lambda}\text{H}$ is successful, the following search for ${}^8_{\Lambda}\text{H}$ hypernucleus will be the most natural aim. We propose to use ${}^9\text{Li}$ beam for such experiment. Also it should be noted that search for ${}^8_{\Lambda}\text{H}$ using pion or kaon beams is even more difficult neither study of ${}^6_{\Lambda}\text{H}$. ${}^9\text{Li}$ beam will be created as a secondary beam when carbon is accelerated. Chain of possible processes is



Lifetimes of ${}^9\text{Li}$ and ${}^8\text{He}$ are of the order of hundred milliseconds what is long enough for the experiment.

Expected production cross sections of the lightest hypernuclei are given in Table 1. New data from the present project will significantly improve the description of the hypernuclei production process. Taking into account these values we have estimated possible counting rate for ${}^4_{\Lambda}\text{H}$ pionic decays equal to 600 events per day in case of ideal Nuclotron operation conditions (spill length 5 s, no intensity pulsations etc.). However, real tests have shown that this value should be reduced few times to 150-200 events per day because spill duration is shorter, we used lower beam intensity on the spectrometer because intensity pulsation causes overlapping of two beam particles inside 50 ns time interval with overlapping of signal amplitudes and so on. Properties of the Nuclotron extracted beam are continuously improved but at this time value of 150-200 events per day is the most realistic. If we suppose that binding energy of ${}^6_{\Lambda}\text{H}$ is low we can expect that its production cross section is of the same order as that of ${}^3_{\Lambda}\text{H}$. Then, one can expect to register 30-40 events of ${}^6_{\Lambda}\text{H}$ per day. But we should recognize that all estimates are based on the idea that coalescence is similar in all hydrogen hypernuclei production processes.

At the next stage of the experiment, **the ${}^6_{\Lambda}\text{He}$ hypernuclei** will be investigated with ${}^6\text{Li}$ beam. The ${}^6_{\Lambda}\text{He}$ will be produced in peripheral Li interactions with carbon target and trigger will be tuned in order to select pionic decays with negative pion and the daughter lithium nucleus emitted from the decay region:



It was established that ${}^6_{\Lambda}\text{He}$ hypernucleus is loosely bound (its neutron separation energy $B = 0.17 \pm 0.10$ MeV). But its lifetime and production cross section were not measured up to now. **It is the ${}^6_{\Lambda}\text{He}$ lifetime measurement which is the first task of the ${}^6_{\Lambda}\text{He}$ experiment.** While ${}^5_{\Lambda}\text{He}$ hypernuclei are investigated very well, it is not so easy to produce ${}^6_{\Lambda}\text{He}$ hypernuclei in other experiments (that is why the study of the

Table 1: Measured and estimated hypernuclei production cross sections. Beam kinetic energy: GeV per nucleon; calculations are from ref. [8]. In ${}^7\text{Li}$ beam on C target we have measured [35] cross section of charge change $\sigma_{cc} = 650 \pm 20\text{mb}$, this value is close to σ_{in} .

Beam	Hyper-nuclei	Energy (GeV)	Cross sec. (μb)	
			Theory	Exp.
${}^3\text{He}$	${}^3_{\Lambda}\text{H}$	5.14	0.03	$0.05^{+0.05}_{-0.02}$
${}^4\text{He}$	${}^3_{\Lambda}\text{H}$	3.7	0.06	< 0.1
	${}^4_{\Lambda}\text{H}$	2.2	0.08	< 0.08
		3.7	0.29	$0.4^{+0.4}_{-0.2}$
${}^6\text{Li}$	${}^3_{\Lambda}\text{H}$	3.7	0.09	$0.2^{+0.3}_{-0.15}$
	${}^4_{\Lambda}\text{H}$	3.7	0.2	$0.3^{+0.3}_{-0.15}$
${}^7\text{Li}$	${}^7_{\Lambda}\text{Li}$	3.0	0.11	< 1
	${}^6_{\Lambda}\text{He}$	3.0	0.25	< 0.5

${}^6_{\Lambda}\text{He}$ was stopped after emulsion experiments). Indeed, in kaon or pion beams ${}^5_{\Lambda}\text{He}$ is produced if a ${}^6\text{Li}$ target is used.

The method of the Coulomb dissociation suggested in refs. [17, 36, 37, 38] will be exploited for the **experimental estimation of the ${}^3_{\Lambda}\text{H}$ and ${}^6_{\Lambda}\text{He}$ binding energy**. This method is interesting from experimental point of view because interactions of hypernuclei “beam” should be investigated.

Study of nonmesonic decays of the ${}^{10}_{\Lambda}\text{Be}$ and ${}^{10}_{\Lambda}\text{B}$ hypernuclei is planned in the present project as well. This study is aimed on **determination of the $\Lambda\text{N} \rightarrow \text{NN}$ weak interaction matrix elements** and implies measurements of the branching ratios $\Gamma_{\alpha\alpha i}^{n(p)}$ for the exclusive decays of the ${}^{10}_{\Lambda}\text{Be}$ and ${}^{10}_{\Lambda}\text{B}$ hypernuclei [20, 39].

In such experiment one should register the chain of decays, for example ${}^{10}_{\Lambda}\text{B}$ which decays without emission of pion (nonmesonic decay) into ${}^{10}_{\Lambda}\text{B} \rightarrow \text{n} + \text{p} + {}^8\text{Be}^*$ with subsequent ${}^8\text{Be}^*$ decay emitting two α 's within a very small angle. Because the two alpha particles and the decay products of the excited hypernuclei are emitted in a very narrow cone, the additional high resolution detectors should be installed to detect the twin alpha particles. Calculations have shown that GEM detectors of $10 \times 10 \text{ cm}^2$ area can solve the problem. Additional trigger counter with thin (1 mm) quartz radiator can suppress by factor of 30-50 the background, coming from the beam nuclei fragmentation in the trigger detectors. Considering spectrometer capability for such an experiment we analyze and test a possibility to install few high resolution trackers, namely scintillating fiber detectors, GEM and microstrip detectors.

3 Spectrometer scheme

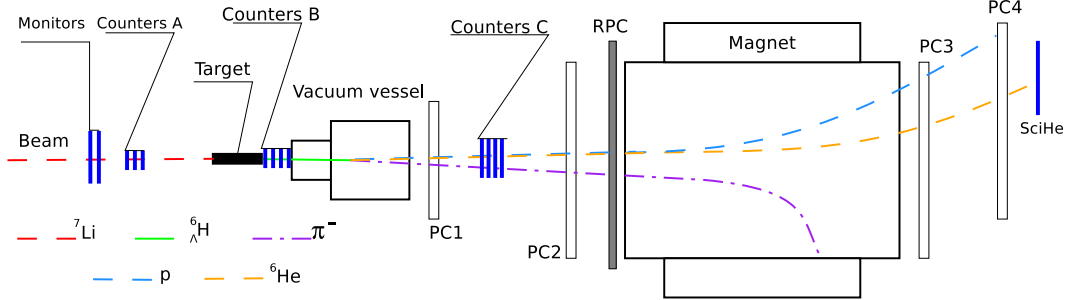
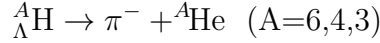


Figure 5: Configuration of the HyperNIS spectrometer. In particular for the search of ${}^6_{\Lambda}\text{H}$ hypernuclei with the ${}^7\text{Li}$ beam (not in scale). Target – carbon $12 \times 3 \times 3$ cm, 20.4 g/cm^2 ; beam monitors; A,B,C – trigger counters; vacuum decay vessel of 55 cm length; the analyzing magnet of 0.6T; PC_{1-4} – proportional chambers, RPC – TOF stations, SciHe – Scintillation counter to confirm registration of ${}^6\text{He}$ nuclei.

Configuration of the spectrometer is presented in Fig. 5. In the ${}^7\text{Li}$ beam nuclei interactions with carbon target (12 cm along the beam and $3 \times 3 \text{ cm}^2$ cross section, 20.4 g/cm^2), when hypernuclei (${}^3_{\Lambda}\text{H}$, ${}^4_{\Lambda}\text{H}$ or ${}^6_{\Lambda}\text{H}$) are produced, pionic decay

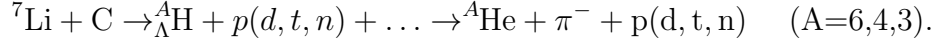


will occur inside the vacuum vessel with rather high probability. The Čerenkov and scintillation counters (trigger detectors B,C correspondingly) are tuned to measure charge difference between hypernucleus and its decay products. Taking into account that resolution of Čerenkov counters is better a block of four Čerenkov counters is used as B detector (as discussed above). Blocks of proportional chambers PC_1 (four chambers $38 \times 38 \text{ cm}^2$) and PC_2 (two chambers $130 \times 80 \text{ cm}^2$) register hits from pion and the daughter nucleus (He), allowing the reconstruction of the decay vertex. In addition, the set of all the proportional chambers (PC_{1-4}) is used to measure momentum of the He nucleus. The chambers PC_{3-4} are of the same size as the chambers PC_2 . With the ${}^7\text{Li}$ beam the full set of the chambers allows detection of the secondary proton (p) or another Li fragment and the momentum separation of the hydrogen hypernuclei daughter nuclei – He isotopes. The scintillation counter SciHe is used to measure and to record signal amplitude at the location where ${}^6\text{He}$ daughter nuclei are expected to separate them between tritium fragments produced together with ${}^4_{\Lambda}\text{H}$ hypernuclei.

4 Experimental method

We underline four main features the method elaborated at JINR. 1.) It is based on an idea to investigate high energy hypernucleus produced due to beam nucleus excitation. 2.) Such hypernucleus decays outside the target what allows one to organize selective trigger and to identify produced isotopes separating daughter nuclei momenta. 3.) Trigger is tuned to find pionic decays of hypernuclei when charge of the daughter nucleus is higher than that of hypernucleus and no physical event can simulate such

charge (and consequently counter signal) relation. 4.) Decay products are forward collimated therefore the spectrometer acceptance is high. 5.) We analyze events when hypernucleus decay vertex is observed in vacuum there no background interaction can simulate the decay. 6.) Momenta of different hypernuclei isotopes are separated by large gaps (like momenta of daughter nuclei what are measured by the spectrometer) therefore it is easy to identify isotopes ${}^3\text{He}$, ${}^4\text{He}$ and ${}^6\text{He}$. In Fig. 6 we present the calculated ${}^3\text{He}$, ${}^4\text{He}$ and ${}^6\text{He}$ momentum distribution for reactions



The next figure 7 shows that just in the case of large possible momentum measurement

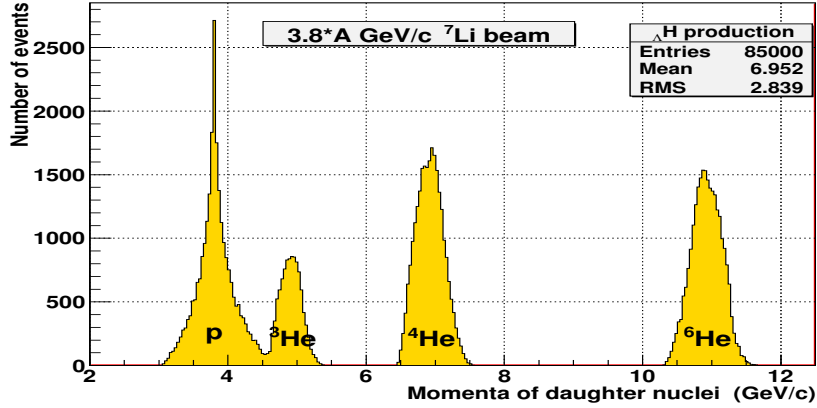


Figure 6: Expected distribution of He (hydrogen hypernuclei daughter nuclei) momenta values divided by their charge. P peak is the calculated momenta of protons produced in the Li fragmentation when ${}^6_{\Lambda}\text{H}$ is produced. The peaks can be easily separated in order to identify different produced hyperhydrogen isotopes.

errors (for example – 2%) peaks are clearly separated.

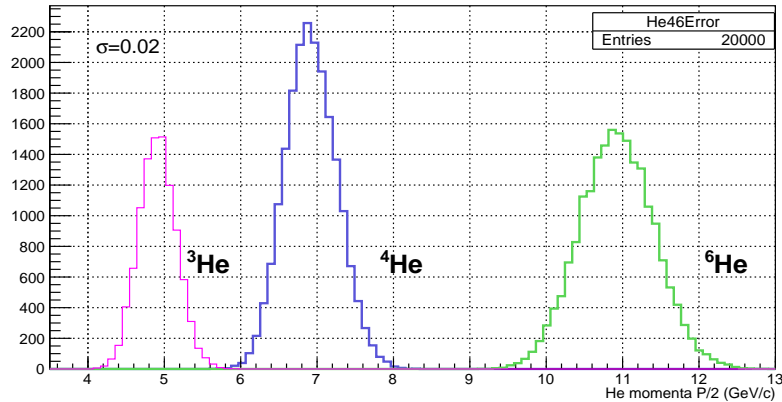


Figure 7: Expected distribution of He (hydrogen hypernuclei daughter nuclei) momenta values divided by their charge in case of 2% momentum error distribution. If ${}^6_{\Lambda}\text{H}$ are produced ${}^4_{\Lambda}\text{H}$ and ${}^6_{\Lambda}\text{H}$ peaks can be easily separated.

In order to measure momenta of relatively slow pions, emitted at relatively large angles, the time-of-flight method will be used. For this purpose a wall of RPC chambers is installed before the analyzing magnet. The detector is effective for approximately 30% of the full pion spectrum and will be used to determine mass of hypernucleus.

Also it should be taken into account that the decay vertices can be found safely if the decay opening angle is not too narrow. We estimate efficiency of vertex reconstruction will be at a level of 90% because opening angles are concentrated at higher values (see Fig. 11). In calculations presented above minimal distance of 3 cm was chosen between He and pion hits in the proportional chambers to be sure that decay vertex position can be reconstructed. However, this cut should be proved experimentally with high statistics of events when two particles leave a thin target. In 2021 two GEM detectors of 40×40 cm size will be obtained and in 2022 installed in order to reduce the number of events rejected due narrow opening angle (see below) and to increase accuracy of hypernuclei decay point location. Thus tracking efficiency will be improved as well. All MC calculations have been done to choose optimal geometry of target and proportional chambers. We should remind that decay products pions and daughter nuclei are forward collimated so that we could find chamber positions to register more than 90% of decay pions. Of course, all daughter nuclei hit proportional chambers.

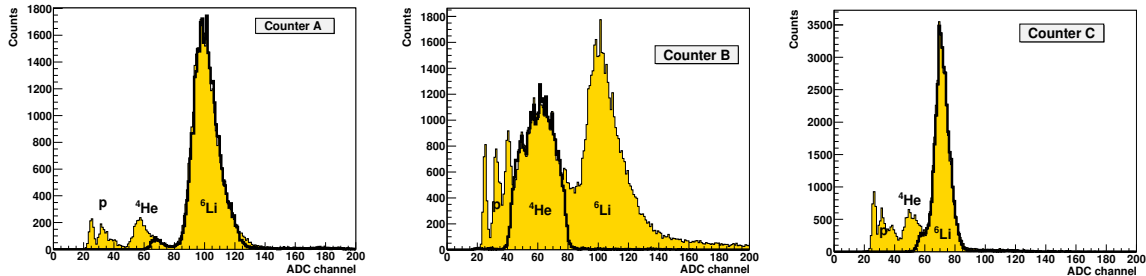


Figure 8: Tuning of trigger (scintillation) counters with ${}^6\text{Li}$ beam for ${}^6_{\Lambda}\text{He}$ production and decay. Example of signal amplitude spectra obtained for counters of beam monitors A, counters of sets B and C correspondingly. Signal amplitude peaks correspond to lithium beam and its fragments from interactions with Al target inserted into beam to produce different lithium fragments: helium, protons, deuterons. Thick line contours part of spectrum determined by discriminators of counters A and C which are tuned to register lithium, counter B – helium. As it was mentioned, scintillation counters B are replaced with Čerenkov counters now.

The trigger aimed to detect the pionic decays of hypernuclei was developed and used successfully in the previous experiment in Dubna [5, 7, 20]. The idea of the trigger is as follows. *When the ${}^6_{\Lambda}\text{H}$ hypernucleus is produced*, the Li nucleus should emit spectator proton while remaining core ${}^6\text{He}$ nucleus is being changed into the ${}^6_{\Lambda}\text{H}$. Each of these two particles have charge equal to 1 (total $Z = 1 + 1$) and hit block of the Čerenkov counters B. Since the counter response is proportional to Z^2 of interacting particle, both particles will create in the Čerenkov B counters the signals proportional to $U = 1^2 + 1^2 = 2$. Less than 2-3% (MC calculations) of associated K^+ (slow, MC calculation) or recoil protons hit the Čerenkov counters B insensitive to slow particles.

Mesonic decay ${}^6_{\Lambda}\text{H} \rightarrow {}^6\text{He} + \pi^-$ results into particles of $Z = 2$ (He) and $Z = 1$ (π^-). The scintillation counters C of minimal size are used in order to register just the

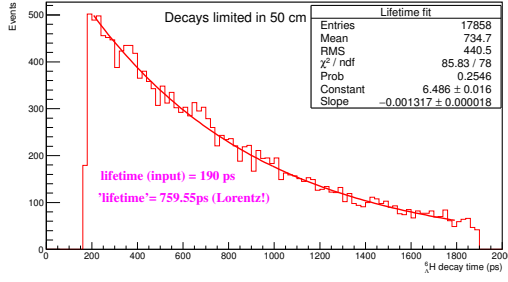


Figure 9: Expected decay time distribution inside of 50 cm distance. Due to Lorentz factor distribution is exponent with 760 ps decay parameter in case of 190 ps lifetime.

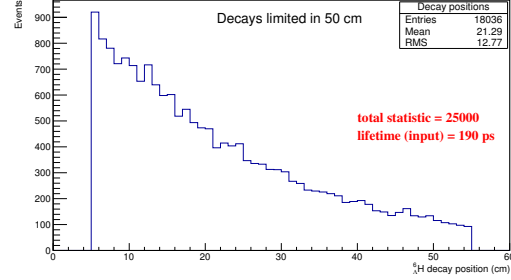


Figure 10: Expected decay points inside of 50 cm decay volume. Since 25000 events analyzed and about 18000 hypernuclei decay inside of 50 cm distance it is 70% of the statistics if the first point is in 5 cm distance from the target.

daughter nuclei. Most pions will miss these counters, and such a condition provides the best amplitude resolution of counters C. As far as the spectator protons are concerned, it is expected that significant fraction of them will hit the counters. However, it is desirable to have a trigger working at full capacity, and therefore, one should ensure that the trigger works efficiently when the C counters have signal proportional to $U = 2^2 = 4$ (only He hits the C), $U = 2^2 + 1^2 = 5$ (proton or pion also hits the counters), and $U = 2^2 + 1^2 + 1^2 = 6$ (all the particles hit the C). Thus, in the counters C one should register signal proportional to $U \geq 4$ if the hydrogen hypernucleus decay takes place but less than $U = 9$ created by Li beam nuclei. Finally, we should underline that in the case of pionic decays the signal registered in the counters C is higher than that of the B while for the majority of the background events the signal in the C is lower than in B. Counters SciHe (see Fig 5) are not a part of the trigger, their signals are recorded and used to check that a ${}^6\text{He}$ was registered in chambers PC3, PC4 not background ${}^3\text{H}$. Some results of trigger tests were presented in [40, 41].

As noted above, significant part of hypernuclei decays just after the target. For example, if one assume ${}^6_{\Lambda}\text{H}$ hypernucleus lifetime equal to 190 ps than ${}^7\text{Li}$ beam of 27 GeV/c momentum (highest value available at the beam line, 3.8 GeV/c per nucleon) produces hypernuclei with lifetime at laboratory frame about 760 ps due to Lorentz factor (see Fig. 9). It can provide a possibility to expect 70% of hypernuclei decays inside of our vacuum vessel if it is situated at a distance of 5 cm from the target (see Fig. 10).

In order to optimize efficiency one should check if short distance between the target and vacuumed decay volume does not cause additional losses due to narrow angle between pion and hypernucleus daughter helium nucleus. Estimates show that a shorter distance between the target and decay volume is the better choice. By increasing this distance we loose statistics not only due to early decays but also due to pions that miss the acceptance of the proportional chambers, while losses due to narrow separation angle stay in 10-16 % interval and therefore are less significant. The distribution of the He-pion separation angle in case of ${}^6_{\Lambda}\text{H}$ decays is presented at Fig. 11, some results of calculated pion distribution at proportional chambers are shown at Fig. 12,13.

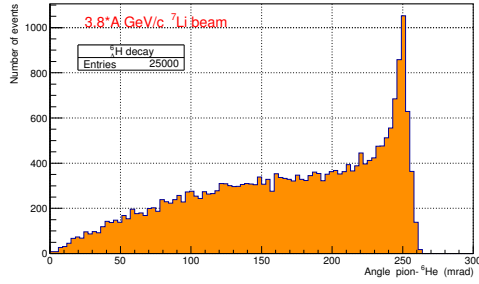


Figure 11: Distribution of calculated pion helium separation angle in ${}^6\text{H} \rightarrow \pi^- + {}^6\text{He}$ decays. About 10-16% decays have separation angles below resolution of the proportional chambers but can be detected using GEM detectors in future experiments.

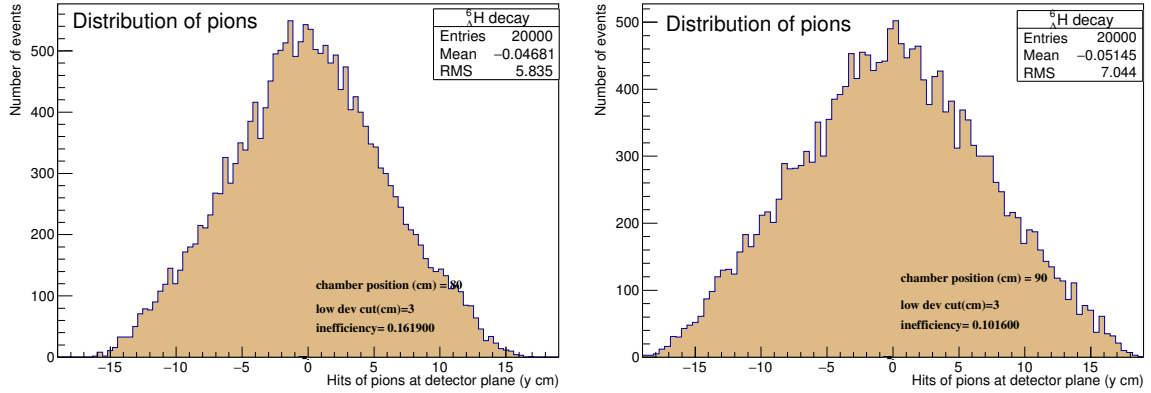


Figure 12: Distribution of pion hits in the proportional chamber situated at 80 cm (left) and 90 cm distance from the beam entrance point of the target. There are no decay pions outside the chamber. Arbitrary large cut of 3 cm distance between He and pion hits is chosen as a limit of inefficiency, the cut in real experimental will be optimized.

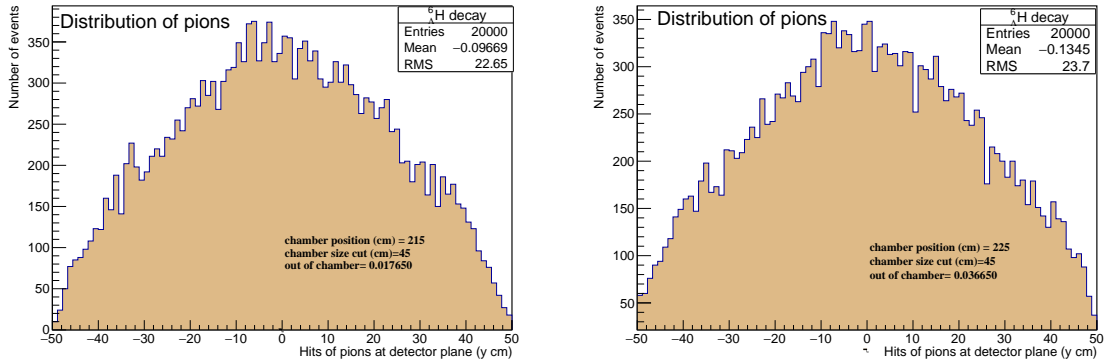


Figure 13: Pion hits at the last chamber to register pions. Geometrical efficiency depends on 10 cm shift of the target position in few percent loss. For the experiment distance of 215 cm is chosen.

5 Last years results and plan for the coming 3 years

During the Nuclotron run 50 the ${}^7\text{Li}$ beam was for the first time delivered to the spectrometer. The obtained beam time was used mostly for tests and tuning of the modernized trigger system in the new counting room (located at new place in the experimental hall). Background suppression factor much higher than 10^4 was reached.

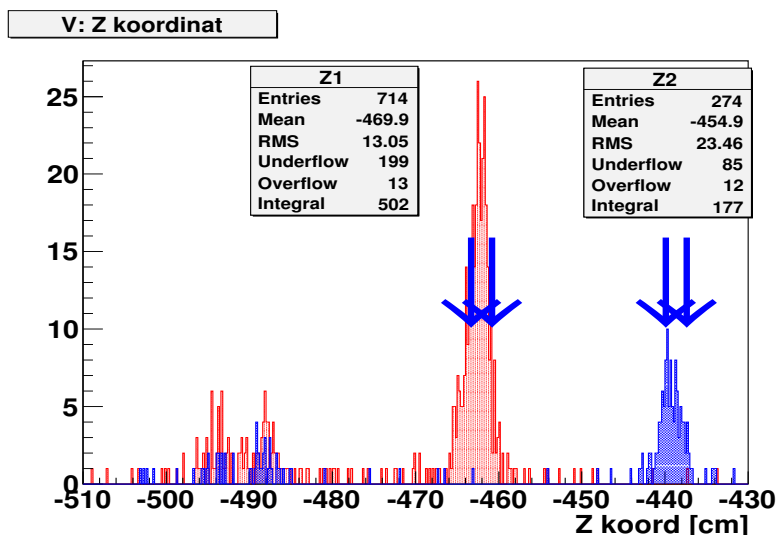


Figure 14: Position of reconstructed ${}^6_\Lambda\text{H}$ along the beam axis - results of a test of alignment codes and vertex reconstruction procedure. The target was placed at two positions (red and blue histograms). The arrows show the edges of the target. Position of two monitor trigger counters are also seen. Vertex position - point of minimal distance d between two tracks ($d < 2\text{mm}$).

Recently, a new tracking upgrade was performed, software is more effective. Some results of tests used MC generated events are presented at Fig. 15,16.

In the last years the Nuclotron upgrade was the highest priority task for the laboratory. Therefore it was necessary to wait until the extracted nuclear beam energy will exceed the hypernuclei production threshold on such a value, which allows to carry out the hypernuclear experiments. Therefore the deuteron beam was used for short test runs in order to calibrate the spectrometer and to test new equipment. Data for proportional chambers alignment were taken, few alignment program codes were developed and investigated, all necessary calculations and fits were carried out. Some results are presented in Fig. 14.

Now the extracted nuclear beam kinetic energy was increased up to 4 GeV/nucleon (well above of the hypernuclei production threshold), the beam line to the HyperNIS spectrometer was tested and the necessary nuclear beam was transported to the spectrometer. Unfortunately, in 2017-2021 Li beam was available only for a short (63 hours) test run, which was used to tune the trigger for hypernuclei detection and to test chambers. This run was too short to start data taking.

On the other hand, the spectrometer was significantly upgraded during the last years. Installation and testing of the time-of-flight detector [42] (RPC wall) before the analyzing magnet in order to determine momentum of pions from decays of hypernuclei

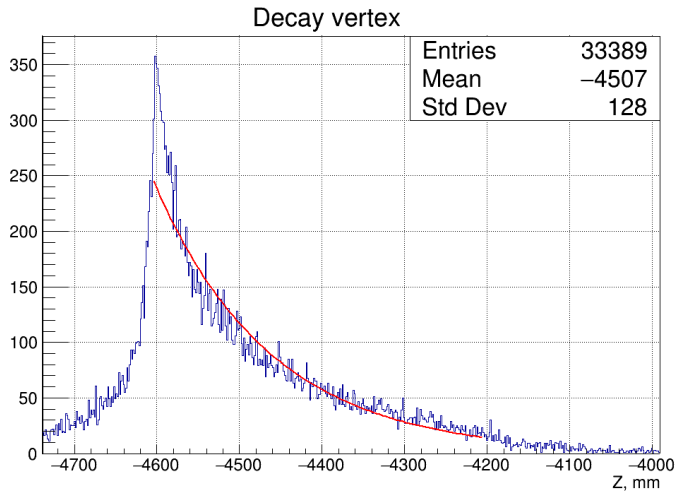


Figure 15: Properly reconstructed decay points allow one to measure lifetime of hypernucleus. $Z=-4600\text{mm}$ is beginning of fiducial decay volume.

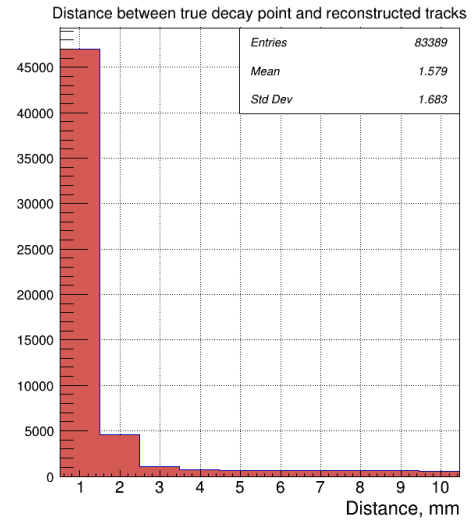


Figure 16: Decay points can be localized into two mm.

(by measuring the time of flight) was a serious step aimed to enhance capability of the spectrometer. New electronic gas supply system (Fig. 17) allows one to stabilize and to improve time resolution. The results of the first tests are presented at Fig. 18. It should be mentioned that similar gas supply (Ethernet computer control possible) was installed for proportional chambers too.



Figure 17: Electronic gas supply system of RPC.

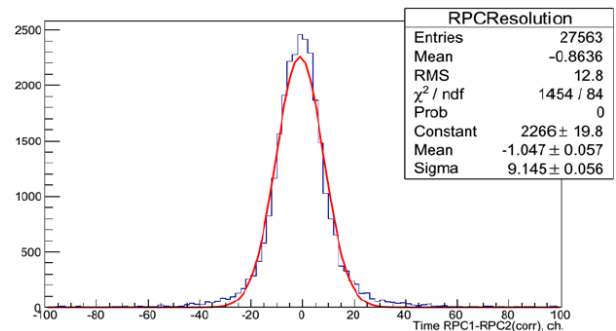


Figure 18: Time resolution of RPC chambers is equal to 180 ps.

But the most important improvement consisted of R&D and production of new front-end electronics for proportional chambers. 200 analog signal cards (32 inputs in each card) were produced in Minsk. The digital part of the FEE cards (see Fig. 19,20) was designed and tested in JINR.

Electronic modules of the trigger system were replaced with new ones too. All modules in VME crate (TQDC modules, data acquisition and service modules as well) and the main DAQ server are new.

Systems of on-line service – the beam control, monitoring of the chamber efficiencies, slow control for the high voltage supply units and others were elaborated, tested and

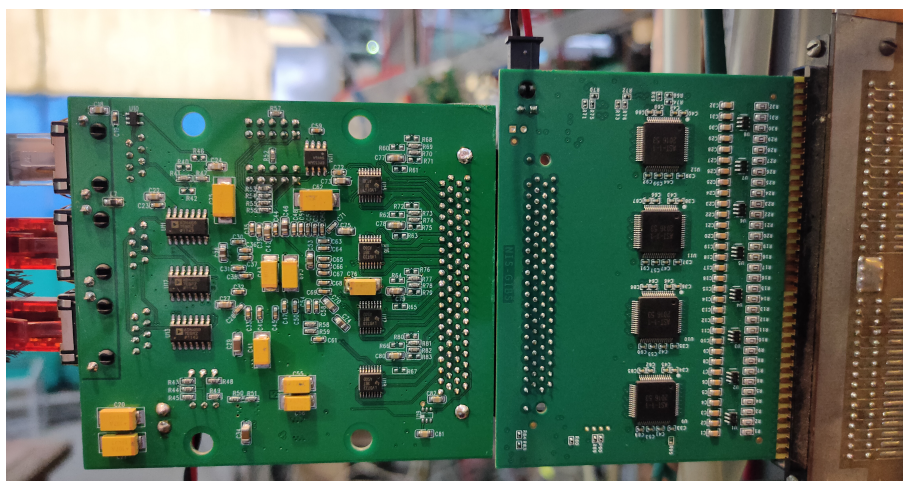


Figure 19: FEE cards: right – chamber output contacts and the analog signal amplifier part, left – the digital part for data processing and transfer.

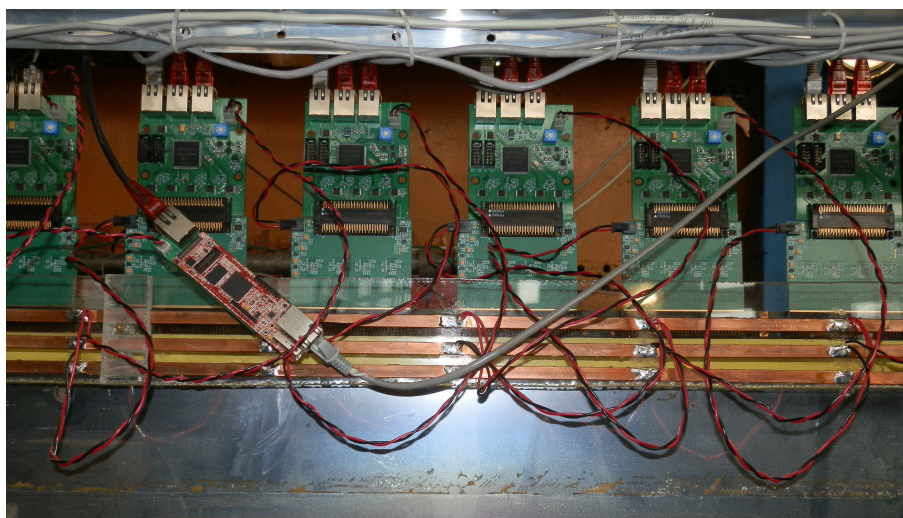


Figure 20: FEE cards on a proportional chamber.

used. Since the beam intensity in the hypernuclei experiments is relatively low ($10^5 - 10^6 s^{-1}$), it was necessary to organize Internet access to the beam control data for the Nuclotron staff. Moreover, taking into account experience of test runs, this system is upgraded from run to run. All data from trigger counters are available in the Nuclotron control room and can be used by the staff to improve the beam tuning.

A new High Voltage supply system was introduced for trigger photomultiplier tubes. It has up to 64 high stability outputs driven by WIENER MPOD crate controller and programs adapted by HyperNIS personal. Proportional chambers are driven using CAEN high voltage supply modules – see Fig. 21. In the time, low voltage systems for proportional chambers were obtained and installed as well. Recently, a block of four

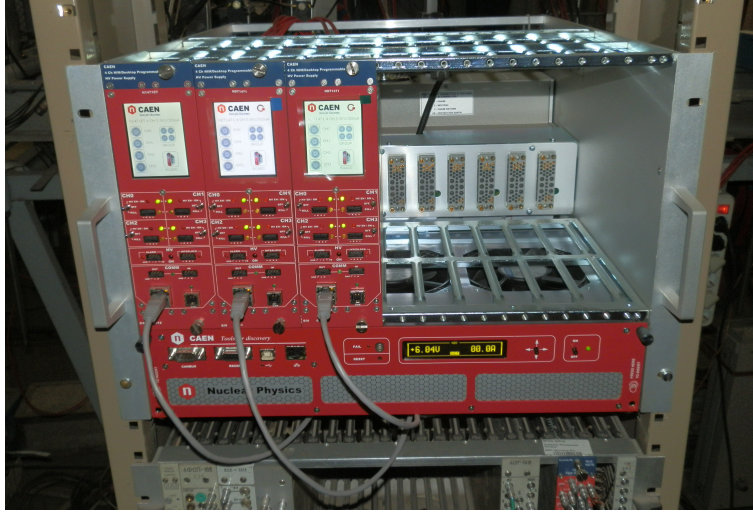


Figure 21: NIM crate with CAEN high voltage power supply for proportional chambers.

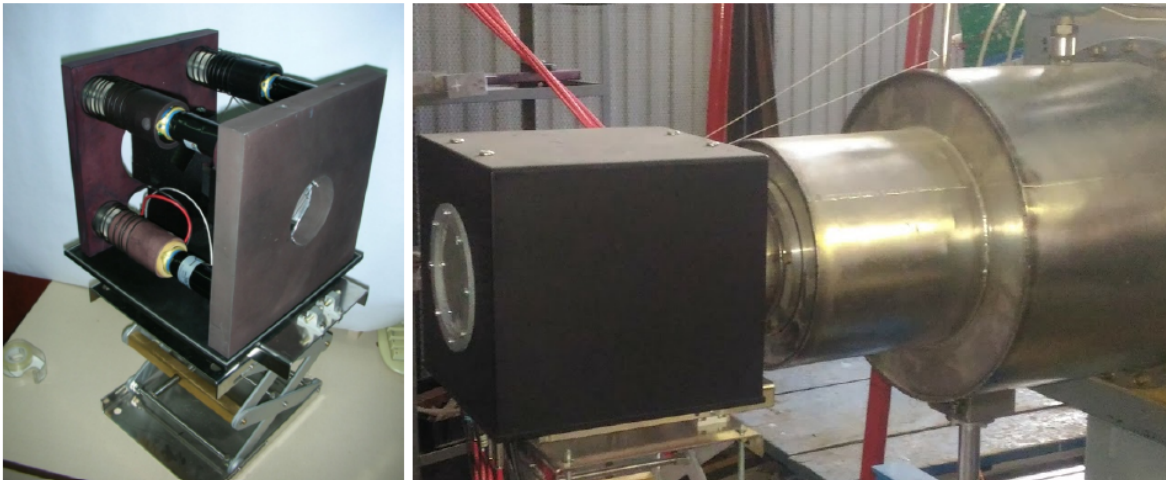


Figure 22: Block of 4 Čerenkov counters with 4 subsequent quartz radiators, 4 mm thick each. On the left side one can see 3 of 4 Electron Tubes 9107B photomultipliers. High density graphite (1.7 g/cm^3) target is placed close to radiators. The block itself is placed close to vacuum vessel (right side of figure).

Čerenkov trigger counters was produced. Carbon target is situated inside of the block close to quartz radiators in order to minimize losses of observed hypernuclei due to decays (approximately 20% of hypernuclei decay along the very first five centimeters after the target). The produced Čerenkov block was tested and amplitude resolution higher than in case of scintillation counter block was obtained (see Fig. 22,23).

To reject possible background of nuclear fragments produced in the trigger counters (tritium first of all) several additional scintillation counters were produced and tested. Planned experiments:

- Focused on the hypernuclear program of the HyperNIS project with use of the d and ${}^7\text{Li}$ beams (the deuteron beam is needed for methodical purposes). In 2022 - two GEM detectors will be installed to improve decay vertex localization.
- The study of hypernucleus ${}^6_{\Lambda}\text{H}$ (years 2022-2023): Search for ${}^6_{\Lambda}\text{H}$, measurements

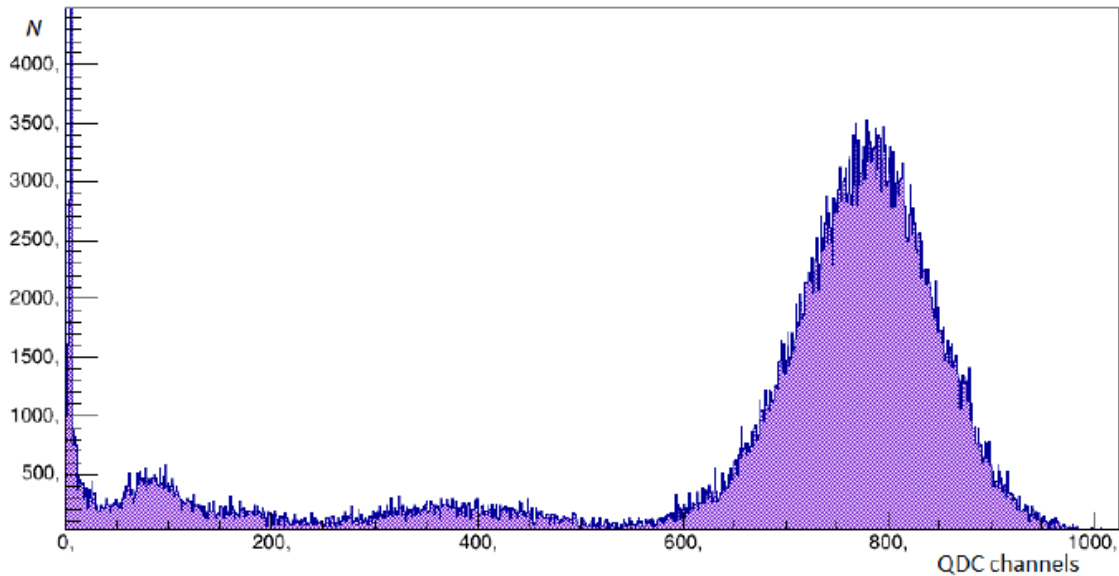


Figure 23: Pulse height distribution of Li beam fragments measured with one of the Čerenkov counters. Clean separation of p, He and Li particles is obtained.

of the lifetime with accuracy of 10-15 ps, production cross section, mass value with accuracy of 1-2 MeV (if the isotope exists). Minimal necessary statistics for these goals is about 500 detected events of the ${}^6_{\Lambda}\text{H}$ production. If production cross section is as low as in case of ${}^3_{\Lambda}\text{H}$ approximately 200 hours of Li beam are necessary.

If the first ${}^6_{\Lambda}\text{H}$ experiments are successful, we will choose the next task: to take 2000 detected events of the ${}^6_{\Lambda}\text{H}$ to check predictions of two lifetimes of isomeric states of the ${}^6_{\Lambda}\text{H}$ or to search for ${}^8_{\Lambda}\text{H}$ hypernucleus using ${}^9\text{Li}$ beam.

- In 2023-2024: study of poorly investigated ${}^6_{\Lambda}\text{He}$ (measurements of the lifetime and production cross section): at least 500 detected events of the ${}^6_{\Lambda}\text{He}$ production are expected.
- In 2023-2024: search for ${}^8_{\Lambda}\text{H}$ hypernucleus; study of nonmesonic decay of medium hypernuclei ${}^{10}_{\Lambda}\text{Be}$ and ${}^{10}_{\Lambda}\text{B}$, tests for measurement of the Coulomb dissociation of ${}^3_{\Lambda}\text{H}$.

The research program of the project should be ended in 2025 year. It is the most important technical result of the project that a new multipurpose magnetic spectrometer with modern detectors and electronics is commissioned and is ready for hypernuclear experiments using extracted Nuclotron beams. The spectrometer will be available for other experiments (tests of detectors).

6 Present status of the apparatus.

After test runs at Nuclotron beam the HyperNIS spectrometer is commissioned. The extracted deuteron and ${}^6\text{Li}$ as well as ${}^7\text{Li}$ beams with kinetic energy of 1.0-3.5 GeV/nucleon and intensity of $10^4 \div 10^5$ 1/sec were used in the test runs of the Nuclotron.

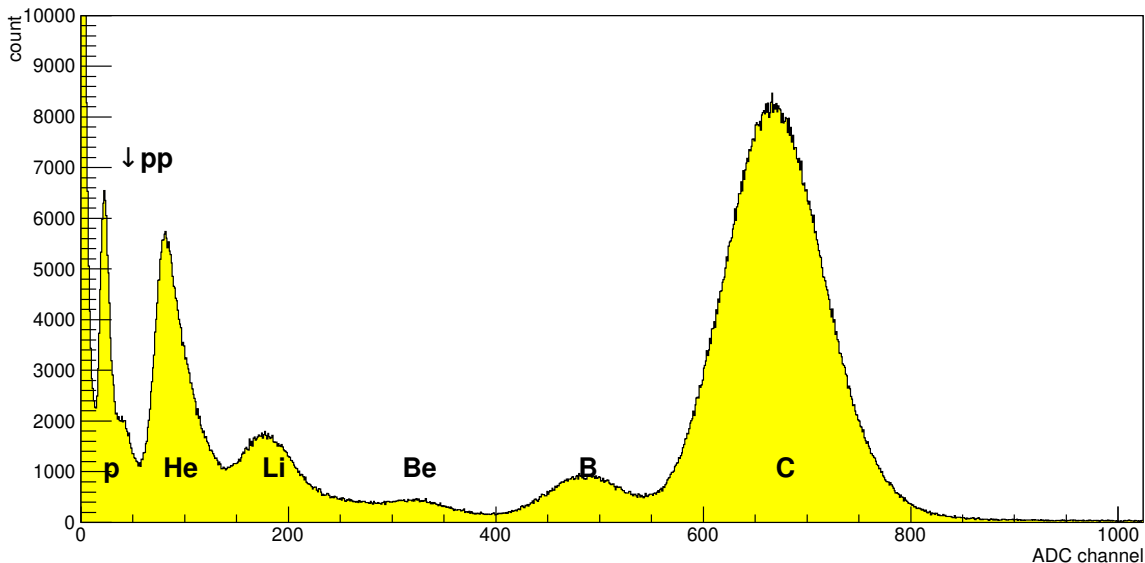


Figure 24: Amplitudes of a trigger scintillation counter measured with carbon beam and mixture of fragments (Al target in the beam).

To provide particles with different electric charges for the trigger tests, the ${}^6\text{Li}$ beam passed through Al target. The composition of the resulted beam after the target is shown in Fig. 8. Similarly, counters response linearity and resolution was tested with carbon beam (see an example of carbon and fragment signal amplitude spectrum in Fig. 24).

It should be noted again that trigger electronics was upgraded in the last few years. Therefore any possibility to have beam was used to test the trigger for hypernuclei study. Even if a beam was not suitable for hypernuclear experiments. While early tests give background suppression of the order of $\sim 2.5 \cdot 10^3$ (see, for example [41]) background rejection of order of $\sim 10^4$ was achieved while a test run with ${}^7\text{Li}$ beam was carried out. It should be added that we use two triggers simultaneously. One of them is aimed to search for hypernuclei production and decay while the second one is organized to check that the spectrometer performance is OK. Since hypernuclei trigger rate is low the second trigger was tuned to detect events every 100 msec when MIP particle crosses counters and proportional chambers. This trigger was used for checking efficiency of all the chambers and for on-line control in the analysis of systematic errors.

The hypernuclei trigger must select events with the following signature: **(i)** “good” incoming beam particles hitting the target are detected, i.e. particles with $Z_{mon} = 3$, for which no other particles appeared within time interval ~ 30 ns before and after it [43]. This selection is done by the “monitor” and “target” subsections of the trigger

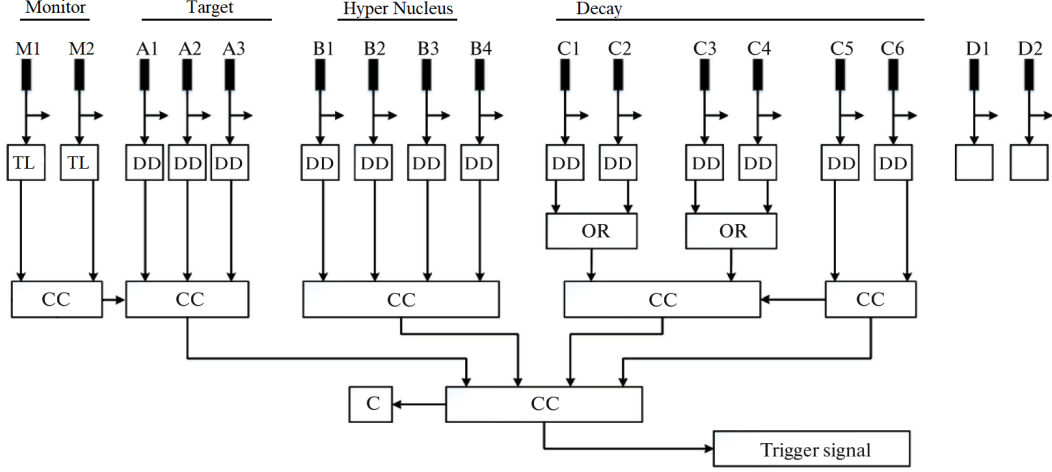
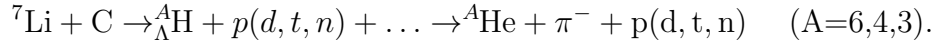


Figure 25: Schematic of reception of the trigger signal: (filled rectangles) PEMs, (DD) differential discriminators, (TL) time locking scheme, (OR) logical adders, (CC) coincidence circuits, and (C) counting circuit.

(Fig. 25) in coincidence; **(ii)** after the target, but before the decay region, a particle with charge $Z = Z_{mon} - 1$ was detected (the “hypernucleus” section in Fig. 25); **(iii)** after the decay region a particle with charge $Z = Z_{mon}$ was detected (the “decay” section in the Fig. 25).

In case of detecting such sequential change of the charge ($3 \rightarrow (1 + 1) \rightarrow \geq 2 < 3$) the trigger generated the signal as shown in Fig. 25 for



Test run with the high energy ($A \times 3.0$ GeV) ${}^7\text{Li}$ beam and renovated trigger system situated in the new counting room showed that the trigger can be tuned to suppress background by a factor much higher than 10^4 [43]. As it was mentioned, 2 GEM detectors are on the way to JINR. Production of GEM detectors was postponed because possible electronics was not ready. Now, advance of the GEM is readout electronics similar to that used at LHEP experiments and it is possible to integrate into our Data acquisition system (DAC). This detector improves hypernuclei decay vertex search algorithm. If GEM is installed between trigger block B and vacuum and registers three particles, we reject the event because all three particles are emitted from the target and do not originate from decay in vacuum. Further, in 2021, installation of two modern gas electron multipliers (CERN production) at the HyperNIS spectrometer is proposed. These detectors GEM1 and GEM2 will have dimensions of active area 400×400 mm, 0.5mm between strips. We propose to install GEM1 before first block of proportional chambers and GEM2 behind it. Both of them will have space resolution near $400 \mu\text{m}$ which allows two times increase of the angular accuracy for the tracks. Furthermore, using these detectors will enlarge the useful statistics by 10% (nearly 15% events contain tracks within a narrow cone and can not be distinguished in the first MWPC now). Also it improves localization of decay vertex point and, consequently, the accuracy of lifetime measurements.

7 Conclusions

The study of properties of the lightest hypernuclei is relevant, has high importance and can be performed in JINR with beams from Nuclotron. Trigger of the HyperNIS spectrometer works with high suppression factor and efficiency. Installing and commissioning of the new FEE allow us to significantly improve tracking efficiency and to carry out the proposed hypernuclear experiments. This can give answers to open questions in hypernuclear physics which are very hard to answering alternative methods and approaches. At present, the HyperNIS spectrometer is tested using beta sources and cosmic muons.

It should be noted that the HyperNIS spectrometer and the beam line can easy be used to test detectors. HyperNIS test runs were used (and can be used in future) to test pixel detectors (TimePix) from Prague (IEAP), microstrip detectors for satellite experiment, etc. TimePix tetsts were carried out together with the Prague team. These tests provided good experience for young Czech researchers. Also several students for JINR were trained. Upgrade of the spectrometer, tuning of new modules and counters, test runs have shown that the HyperNIS team is ready to achieve proposed aims.

Milestones:

- Year 2021: production of two GEM detectors, installation.
- Year 2022: search for the ${}^6_{\Lambda}\text{H}$ using proportional chambers with new readout electronics.
- If search for ${}^6_{\Lambda}\text{H}$ is successful, start of ${}^8_{\Lambda}\text{H}$ experiment with ${}^9\text{Li}$ beam. The study of hypernucleus ${}^6_{\Lambda}\text{H}$ (lifetime with accuracy of 10-15 ps, production cross section, mass value within 1-2 MeV errors) in 2023-2024.
- The study of ${}^6_{\Lambda}\text{He}$ (lifetime, production cross section) and the study of nonmesonic decay of medium heavy nuclei ${}^{10}_{\Lambda}\text{Be}$ and ${}^{10}_{\Lambda}\text{B}$ and Coulomb dissociation of ${}^3_{\Lambda}\text{H}$ depends on NICA fixed target experiment capability.

The results of the first experiments will guide to the next tasks. Therefore the time table can be changed, for example, to search for ${}^8_{\Lambda}\text{H}$ in case of successful ${}^6_{\Lambda}\text{H}$ experiment.

References

- [1] M.Agnelo et al., Phys.Rev.Lett. 108 (2012) 042501.
- [2] E.Botta, Nucl. Phys. **A914** 2013, 119.
- [3] M.Agnello et al., Nucl. Phys. **A881** 2012, 269.
- [4] H.Sugimura et al., J-PARC E10 Collaboration, Phys. Lett. B729 (2014) 39.
- [5] A.U.Abdurakhimov et al., Nuovo Cim. A102, (1989) 645.
- [6] S.A.Avrachenko et al., Communication of JINR, Dubna, 1991.
- [7] S.Avrachenko et al. Nucl. Phys. **A547** 1992, 95c.
- [8] H.Bandō et al., Nucl. Phys. A501, (1989) 900.

- [9] H.Bandō, T.Motoba and J.Žofka, Int. J. Mod. Phys. A5, (1990) 4021.
- [10] Y.Xu,... Proc. 12th Int. Conf. on Hypernuclear and Strange Particle Physics (HYP2015) JPS Conf. Proc. 17, 021005 (2017), <https://doi.org/10.7566/JPSCP.17.021005>.
- [11] S.Piano,...Proc. 12th Int. Conf. on Hypernuclear and Strange Particle Physics (HYP2015) JPS Conf. Proc. 17, 021004 (2017), <https://doi.org/10.7566/JPSCP.17.021004>.
- [12] C.Rappold, T.Saito, Proc. 12th Int. Conf. on Hypernuclear and Strange Particle Physics (HYP2015) JPS Conf. Proc. 17, 021003 (2017), <https://doi.org/10.7566/JPSCP.17.021003>.
- [13] H. Kamada, J. Golak, K. Miyagawa, H. Witala, W. Glöckle: Phys. Rev. C 57 (1998) 1595.
- [14] T. Motoba, et al.: Nucl. Phys. A 534 (1991) 597.
- [15] B. Donigus for the ALICE Collaboration, AIP Conference Proceedings 2130, 020017 (2019); <https://doi.org/10.1063/1.5118385> Published Online: 25 July 2019
- [16] L. Adamczyk et al. (STAR Collaboration) Phys. Rev. C 97, 054909 (2018)
- [17] S.A.Avramenko et al., Nucl.Phys. A585, (1995) 91c.
- [18] T.Saito, *Proceedings of the IX International Conference on Hypernuclear and Strange Particle Physics (HYP06), 2006, Mainz*, ed. by J.Pochodzalla and Th.Walcher (SIF and Springer-Verlag Berlin Heidelberg 2007) p.171.
- [19] C.Rappold et al., Nucl.Phys. A913 (2013) 170.
- [20] Yu.A.Batusov, J.Lukstins, L.Majling and A.N.Parfenov, Physics of Elementary Particles and Atomic Nuclei 36, (2005) 169.
- [21] Z. Azoumanian et al., Astrophys. J. Suppl. 235, (2018) 37, J. Antoniadis et al., Science 340, (2013) 1233232, H. T. Cromartie et al., Nature Astronomy 10.1038 (2019)
- [22] D.Logoteta, I.Vidana, and I.Bombaci, arXiv:1906.11722, Eur. Phys. J. A55 (2019) Article 207
- [23] Proc. 12th Int. Conf. on Hypernuclear and Strange Particle Physics (HYP2015) JPS Conf. Proc. 17, 011007 (2017), <https://doi.org/10.7566/JPSCP.17.011007>.
- [24] T.Nagae, Nucl. Phys. **A942** 2013, 559.
- [25] R.H. Dalitz and R. Levi Setti, Nuovo Cimento 30 (1963) 498.
- [26] Y. Akaishi and T. Yamazaki, Frascati Phys. Ser. XVI (1999) 59.
- [27] A. Gal and D.J. Millener, Phys. Lett. B725 (2013) 445.
- [28] E. Hiyama, S. Ohnishi, M. Kamimura and Y. Yamamoto, Nucl. Phys. A908 (2013) 29.
- [29] A.Gal, D.J.Millener, arXiv:1305.6716v4 [nucl-th] 28 Aug 2013.
- [30] B.F.Gibson, I.R.Afnan, Nucl. Phys. A (2014), in press.
- [31] L.Majling, Nucl. Phys. A585, (1995) 211c.
- [32] L.Majling, *Proceedings of the IX International Conference on Hypernuclear and Strange Particle Physics (HYP06), 2006, Mainz*, ed. by J.Pochodzalla and Th.Walcher (SIF and Springer-Verlag Berlin Heidelberg 2007) p.149.
- [33] K.S.Myint and Y.Akaishi, Progr. Theor. Phys. Suppl. 146, (2002) 599.
- [34] S.Shinmura et al., J. Physics G: Nucl. Part. Phys. 28, (2002) L1.
- [35] S.A.Avramenko et al., Communication of JINR P1-91-206, Dubna, 1991.
- [36] J.Lukstins, Nucl. Phys. A691, (2001) 491c.

- [37] S.V.Afanasiev et al., *Proceedings of the IX International Conference on Hypernuclear and Strange Particle Physics (HYP06), 2006, Mainz*, ed. by J.Pochodzalla and Th.Wacher (SIF and Springer-Verlag Berlin Heidelberg 2007) p.165.
- [38] M.V.Evlanov et al., Nucl. Phys. A632, (1998) 624; M.V.Evlanov et al., *Particles and Nuclei Letters* 105, (2001) 5.
- [39] L.Majling and Yu.Batusov, Nucl. Phys. A691, (2001) 185c.
- [40] R.A.Salmin, O.V.Borodina, A.I.Maksimchuk, V.L.Rapatsky, talks at the LHE JINR Seminar on relativistic nuclear physics, June 06, 2007.
- [41] V.D.Aksinenko et al, *Proceedings of International Baldin seminar on high energy physics problems "Relativistic Nuclear Physics and Quantum Chromodynamics", Dubna, September 29 - October 4, 2008*, JINR, Dubna, 2008, p.155.
- [42] A. V. Averyanov, S. A. Avramenko, V. D. Aksinenko, A. N. Baeva, S. V. Gertsenberger, A. I. Golokhvastov, A. M. Korotkova, D. O. Krivenkov, J. Lukstins, A. I. Maksimchuk, E. A. Matyushina, O. V. Okhrimenko, N. G. Parfenova, S. N. Plyashkevich, R. A. Salmin, E. A. Strokovsky, and A. A. Feschenko, *Time-of-Flight System of HyperNIS Spectrometer*, ISSN 1547-4771, *Physics of Particles and Nuclei Letters*, 2019, Vol. 16, No. 6, pp. 796–806.
- [43] A. V. Averyanov, S. A. Avramenko, V. D. Aksinenko, A. N. Baeva, S. V. Gertsenberger, A. I. Golokhvastov, A. M. Korotkova, D. O. Krivenkov, J. Lukstins, A. I. Maksimchuk, E. A. Matyushina, O. V. Okhrimenko, N. G. Parfenova, S. N. Plyashkevich, R. A. Salmin, E. A. Strokovsky, and A. A. Feschenko, *Trigger System of the HyperNIS Experiment*, ISSN 1547-4771, *Physics of Particles and Nuclei Letters*, 2019, Vol. 16, No. 6, pp. 826–834.